Ensemble forecasting of typhoon rainfall and floods over a mountainous watershed in Taiwan ☆

Ling-Feng Hsiao [a], Ming-Jen Yang [a,b,*], Cheng-Shang Lee [a,c], Hung-Chi Kuo [a,c], Dong-Sin Shih [a], Chin-Cheng Tsai [a], Chieh-Ju Wang [a], Lung-Yao Chang [a], Delia Yen-Chu Chen [a], Lei Feng [a], Jing-Shan Hong [d], Chin-Tzu Fong [d], Der-Song Chen [d], Tien-Chiang Yeh [d], Ching-Yuang Huang [a,b], Wen-Dar Guo [a], Gwo-Fong Lin [a,e]

[a] Taiwan Typhoon Flood Research Institute, National Applied Research Laboratories, Taipei, Taiwan
[b] Department of Atmospheric Sciences, National Central University, Chung-Li, Taiwan
[c] Department of Atmospheric Sciences, National Taiwan University, Taipei, Taiwan
[d] Central Weather Bureau, Taipei, Taiwan
[e] Department of Civil Engineering, National Taiwan University, Taipei, Taiwan

ARTICLE INFO

SUMMARY

In this study, an ensemble meteorological modeling system is one-way coupled with a hydrological model to predict typhoon rainfall and flood responses in a mountainous watershed in Taiwan. This ensemble meteorological model framework includes perturbations of the initial conditions, data analysis methods, and physical parameterizations. The predicted rainfall from the ensemble meteorological modeling system is then used to drive a physically distributed hydrological model for flood responses in the Lanyang basin during the landfall of Typhoon Nanmadol (2011). The ensemble forecast provides track forecasts that are comparable to the operational center track forecasts and provides a more accurate rainfall forecast than a single deterministic prediction. The runoff forecast, which is driven by the ensemble rainfall prediction, can provide uncertainties for the runoff forecasts during typhoon landfall. Thus, the ensemble prediction system provides useful probability information for rainfall and runoff forecasting.

© 2013 The Authors. Published by Elsevier B.V. All rights reserved.

1. Introduction

Typhoons are one of the most important severe weather systems in Taiwan. The heavy rainfall and strong winds that are associated with typhoons can cause tremendous damage in Taiwan. On average, three to four typhoons make landfall in Taiwan each year. Due to the disasters and high social impacts that result from typhoons, accurate typhoon forecasting is a priority of operational weather forecast centers in the western North Pacific, especially in Taiwan.

Typhoon track forecasts are primarily based on the guidance from numerical weather prediction (NWP) models. However, the NWP models are inherently limited due to the predictability limits that result from the intrinsic chaotic nature of the atmospheric system. Consequently, future weather states are sensitive to small errors in the initial state (Lorenz, 1963). Errors in initial conditions (ICs) and in model physics result in forecast uncertainties in the NWP models (Tribbia and Baumhefner, 1988). One approach for reducing these uncertainties is the use of ensemble forecasting (Epstein, 1969). An ensemble forecast that explicitly represents these uncertainties would provide useful quantitative information regarding the probability of the weather systems (Murphy, 1990).

Convection-allowing models use grid sizes that are small enough to simulate convective processes explicitly. In contrast, the models with coarse horizontal grid sizes must use a cumulus parameterization scheme to represent the effects of subgrid-scale convective processes (Weisman et al., 1997; Kain et al., 2006). Kain et al. (2008), Weisman et al. (2008), and Clark et al. (2010) indicated that the convection-allowing NWP models with fine horizontal grid spacing provide value-added predictions for severe convective storms and their associated heavy rainfall.

Several operational centers, including the European Centre for Medium-Range Weather Forecasts (ECMWF), the National Centers for Environmental Prediction (NCEP), the Japan Meteorological Agency (JMA), and the United Kingdom Meteorological Office (UKMO), provide valuable operational ensemble predictions at a
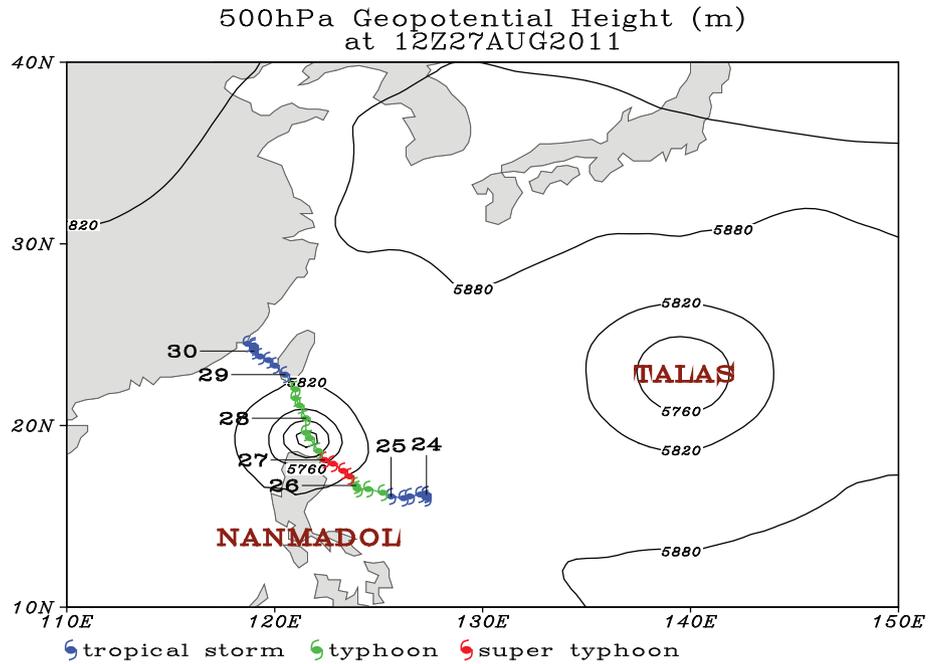
Fig. 1. 500-hPa geopotential height at 1200 UTC 27 August 2011 from the analysis of NCEP GFS (with a contour interval of 60 hPa). CWB best-track positions for Typhoon Nanmadol are plotted every 6 h from 1200 UTC 23 to 1800 UTC 30 August with labels indicating the date of August 2011 at 0000 UTC.
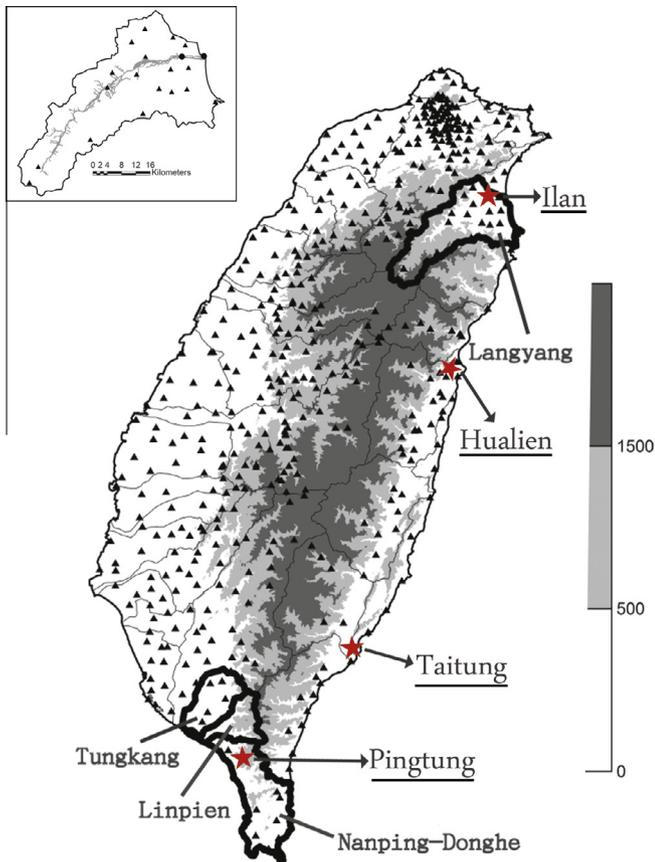

Fig. 2. Taiwan topography with gray shading at 500 and 1500 m. 512 rainfall stations including conventional and automatic rainfall and Meteorological Telemetry System stations (triangle symbols) are plotted. Contours indicate the boundaries of 33 river basins on Taiwan. Four basins (dark black contours) are the targeted areas discussed in Sections 5 and 6. The insert illustrates the Lanyang basin over northeastern Taiwan with rain-gauge (triangle symbols) and flow (closed circles) stations. Star symbols denote the cities of Ilan, Hualien, Taitung, and Pingtung.
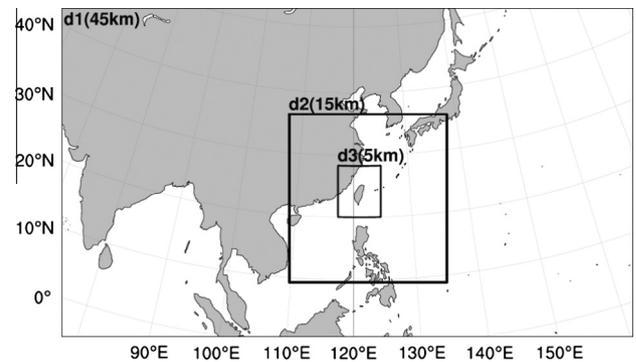

Fig. 3. Three nested domains for ensemble members.

global scale (Buizza, 2007; Bowler et al., 2008; Yamaguchi et al., 2009; Hamill et al., 2011). Regional scale ensemble prediction systems have been developed in research and operational modes to address the need for detailed and high-impact weather forecasting with higher spatial resolution (Du et al., 2009; Yamaguchi et al., 2009; Clark et al., 2010).

Previous studies have indicated that ensemble forecasting is promising for predicting tropical cyclones (hurricanes/typhoons). Krishnamurti et al. (1997) examined the ensemble forecasts of three hurricanes in 1979, and obtained useful track forecasts with reduced spread. Yamaguchi et al. (2009) showed that the ensemble mean track forecasts for typhoons in the western North Pacific in 2007 had a 40-km error reduction in the 5-day forecasts compared to the deterministic model forecast. Snyder et al. (2010) demonstrated that the NCEP global ensemble forecast system was significantly more accurate for forecasting Atlantic tropical cyclone (TC) tracks between August and September in 2006.

Although these ensemble forecasting results are encouraging, the ensemble meteorological forecasting system has not been coupled with a hydrological model for typhoon-related flood forecasting for mountainous watersheds in Taiwan. The hydrological responses of most watersheds in Taiwan are fast and complicated

Table 1
Model configuration for ensemble members. The table elements from initial conditions (ICs), lateral boundary conditions (LBCs) and various physical parameterizations are described in the text.

| Ensemble member	Model	ICs				LBCs	Cumulus scheme	Microphysics scheme	Boundary layer
01	WRF	Partial cycle	3DVAR (CV5 + OL)	Bogus		NCEP GFS	GD	Goddard	YSU
02	WRF	Partial cycle	3DVAR (CV5 + OL)	Bogus		NCEP GFS	G3	Goddard	YSU
03	WRF	Partial cycle	3DVAR (CV5 + OL)	Bogus		NCEP GFS	BMJ	Goddard	YSU
04	WRF	Partial cycle	3DVAR (CV5)	Bogus		NCEP GFS	KF	Goddard	YSU
05	WRF	Partial cycle	3DVAR (CV5 + OL)	Bogus	Two-way interaction	NCEP GFS	KF	Goddard	YSU
06	WRF	Cold start	3DVAR (CV5 + OL)	Bogus		NCEP GFS	KF	Goddard	YSU
07	WRF	Cold start	3DVAR (CV5 + OL)	Bogus		NCEP GFS	GD	Goddard	YSU
08	WRF	Cold start	3DVAR (CV5 + OL)	Bogus		NCEP GFS	G3	Goddard	YSU
09	WRF	Cold start	3DVAR (CV5 + OL)	Bogus		NCEP GFS	BMJ	Goddard	YSU
10	WRF	Partial cycle	3DVAR (CV3)			NCEP GFS	KF	Goddard	YSU
11	WRF	Partial cycle	3DVAR (CV5 + OL)	Bogus		NCEP GFS	KF	Goddard	YSU
12	WRF	Partial cycle	3DVAR (CV3)			CWB GFS	KF	Goddard	YSU
13	WRF	Cold start	3DVAR (CV3)	Bogus		NCEP GFS	KF	Goddard	YSU
14	WRF	Cold start	3DVAR (CV5)	Bogus		NCEP GFS	KF	Goddard	YSU
15	WRF	Cold start	3DVAR (CV5)	Bogus	Two-way interaction	NCEP GFS	KF	Goddard	YSU
16	WRF	Cold start	NODA			NCEP GFS	KF	WSM5	YSU
17	MM5	Cold start	NODA			NCEP GFS	Grell	Goddard	MRF
18	MM5	Cold start	4DVAR	Bogus		NCEP GFS	Grell	Goddard	MRF
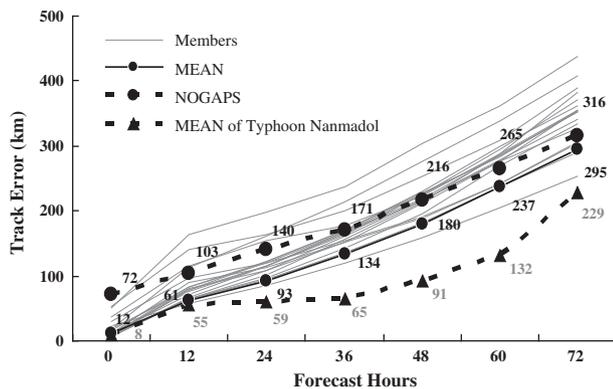
Fig. 4. Mean track forecast errors of 18 ensemble members (gray line), ensemble mean (closed circle with solid line), and the NOGAPS forecasts (closed circle with dash line) from 21 typhoons over the Western North Pacific Ocean in 2011. Triangle with dash line denotes the ensemble mean track error for Typhoon Nanmadol.

due to the steep slopes of the Central Mountain Range (CMR). Heavy rainfall, particularly during typhoon landfall, may cause downstream flooding and peak water flow within a few hours due to fast basin flood responses. However, typhoons are also an important water resource for Taiwan. Accurate runoff forecasts are important for providing accurate information regarding water resource use to reservoir managers and policy makers and for making reservoir storage and discharge decisions.

Successful simulation of a basin flood with a hydrological model depends on accurate rainfall information (Zhang and Smith, 2003; Li et al., 2005). Lee et al. (2000), Hsu et al. (2003), and Li et al. (2005) used a physically distributed hydrological model to simulate discharge from the Tanshui river in Taiwan. In this study, the Lanyang creek basin, which is located in northeastern Taiwan, was selected as the target area for watershed modeling because it lies in the pathway of many typhoons that pass near Taiwan. This watershed has a short hydrological response time due to its steep topography. The one-way coupled hydrometeorological approach with rainfall forcing from an ensemble mesoscale modeling system was used in this study to predict rainfall and flooding during the landfall of Typhoon Nanmadol (2011).

Typhoon Nanmadol produced heavy rainfall that resulted in agricultural and industry damage and the loss of many lives. Nanmadol became a tropical storm at 1200 UTC 23 August 2011 as it moved westward to northwestward along the southern edge of the subtropical high. Following landfall in the northeastern Philippines at 0000 UTC 27 August, its intensity was reduced from category 3 to category 2 [based on the Saffir–Simpson hurricane scale (Simpson, 1974)]. Nanmadol then moved north–northwestward due to the westward extension of the subtropical high before making landfall in southeastern Taiwan on 28 August (Fig. 1). After Nanmadol passed over Taiwan, it rapidly weakened before dissipating over the Taiwan Strait.
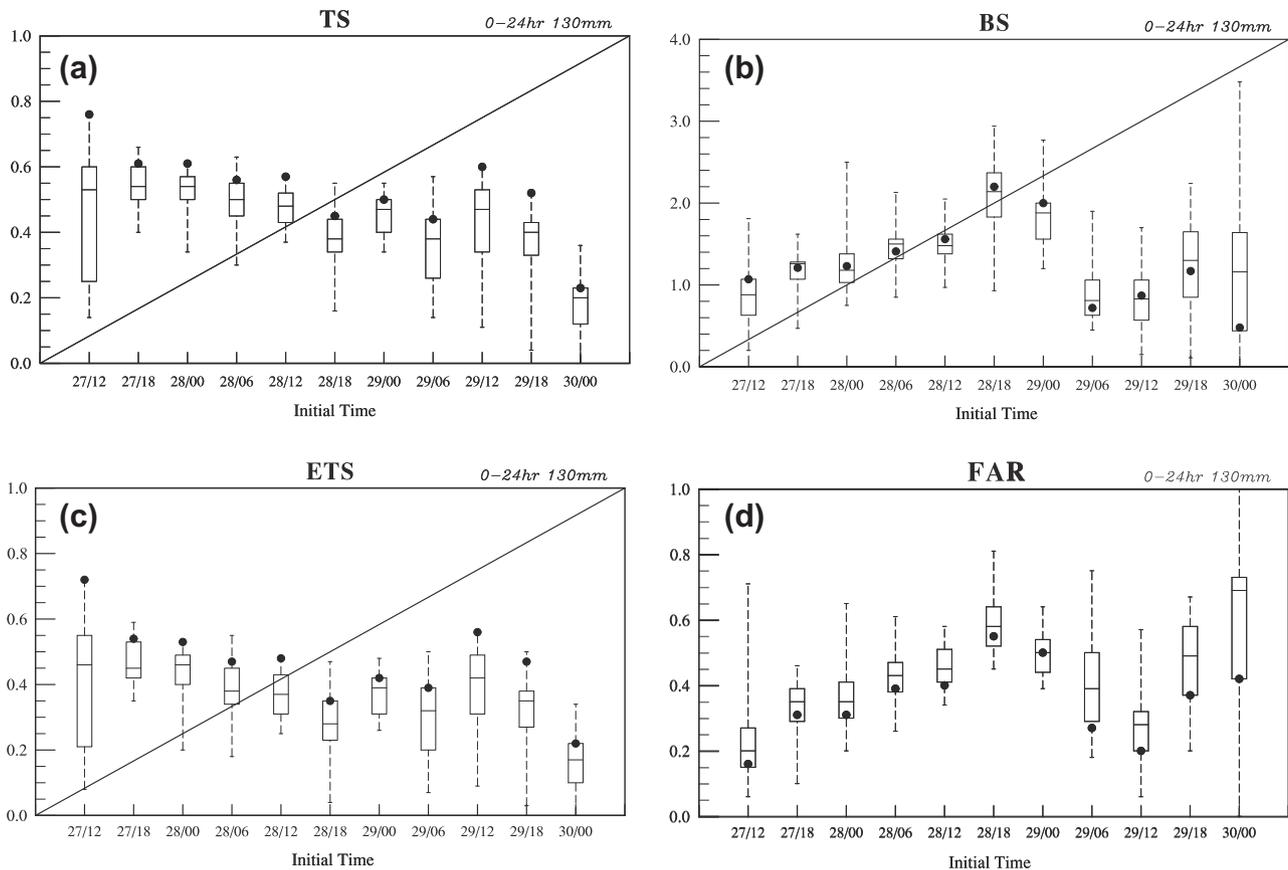
Fig. 5. Box-and-whisker plot of (a) threat score (TS), (b) bias score (BS), (c) equitable threat score (ETS), and (d) false alarm rate (FAR) for 24-h accumulated rainfall forecast of the 18 individual members at the 130-mm threshold for Typhoon Nanmadol from 1200 UTC 27 to 0000 UTC 30 August during which the CWB issued typhoon warnings. Values of the ensemble mean of rainfall forecast are indicated with dots. The box-and-whisker plot is interpreted as follows: the middle line shows the median value; the top and bottom of the box show the upper and lower quartiles (i.e., 75th and 25th percentile values); and the whiskers show the minimum and maximum values.

From 1200 UTC 27 August to 0000 UTC 30 August, the Central Weather Bureau (CWB) of Taiwan issued typhoon warnings for heavy rainfall and strong winds. Two major rainfall maxima occurred in eastern and southern Taiwan, respectively. Prior to Nanmadol's landfall in southeastern Taiwan, the main rainfall centers were located in the eastern Taiwan with the 3-day accumulations of 568, 520, and 308 mm in the cities of Hualien, Taitung, and Ilan, respectively. In addition, a rainfall maximum occurred in Pingtung County with a 3-day accumulation of 1080 mm. In Taiwan, a total property loss of 100 million Taiwan dollars (3.3 million US dollars) resulted from Typhoon Nanmadol.

Hydrometeorological observations, the ensemble meteorological modeling system, the hydrological model, and the prediction skill measures for Nanmadol are described in Section 2. The track verifications for the ensemble forecasts for 21 typhoons and for Typhoon Nanmadol in 2011 are discussed in Section 3. The rainfall forecast verifications and flood simulations for Nanmadol are discussed in Sections 4 and 5, respectively. Finally, concluding remarks are provided in Section 6.

2. Data and methods

2.1. Observations

Rainfall forecasts were verified at all of the 512 automatic rain-gauge stations on the Taiwan Island (Fig. 2). In addition, the rainfall forecasts by ensemble members were interpolated to the rain-gauge stations using the Kriging technique (Bras and Rodriguez-Iturbe, 1985). Lanyang stream is the main river that drains into this

watershed, which has rain-gauge sites and two flow stations (Fig. 2 insert).

2.2. Model setups

2.2.1. Mesoscale meteorological models: WRF and MM5

Two mesoscale models systems were used in the ensemble, including the Weather Research and Forecasting (WRF) model and the fifth-generation Pennsylvania State University–National Center for Atmospheric Research (PSU–NCAR) Mesoscale Model (MM5). The WRF modeling system is a mesoscale forecast and data assimilation system that is designed to advance atmospheric research and operational prediction (Skamarock et al., 2008). The dynamics solver of the Advanced Research WRF model (WRF-ARW) integrates the compressible and nonhydrostatic Euler equations. The vertical coordinate is a terrain-following, hydrostatic-pressure coordinate with the model top at a constant pressure surface (30 hPa). In addition, the WRF contains an advanced physics package and a variational data assimilation (WRF-VAR) system that ingests many types of observations to better represent the initial conditions.

The MM5 model is a limited-area, terrain-following, and sigma-coordinate model that is designed to predict mesoscale weather phenomena. The basic MM5 model structure, including vertical and horizontal grids and finite-difference equations, is described by Grell et al. (1995).

2.2.2. Ensemble configuration

The ensemble meteorological modeling system uses three nested domains (Fig. 3). The outermost domain has 221 × 127 grid
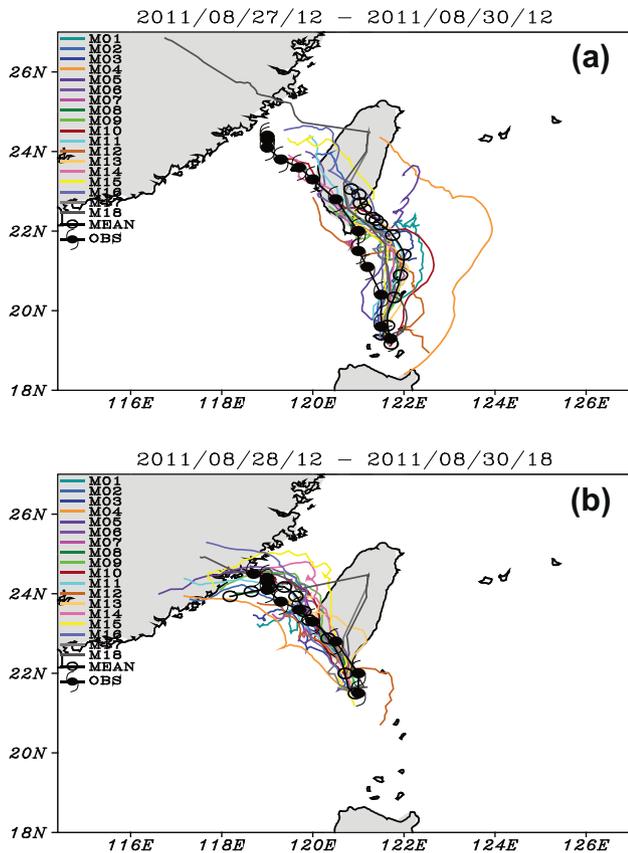
Fig. 6. Six-hourly tracks of Typhoon Nanmadol from the CWB best-track analysis (typhoon symbols), ensemble mean (open circles) and each ensemble member (colored lines) for (a) a 72-h forecast starting from 1200 UTC 27 August and (b) a 54-h forecast starting from 1200 UTC 28 August. (For interpretation of the references to color in this figure legend, the reader is referred to the web version of this article.)

points in the east–west and north–south directions with a horizontal grid size of 45 km. This domain covers most of Asia and the western North Pacific Ocean. The middle and inner domains have 183 × 195 and 150 × 180 grid points with horizontal grid sizes of 15 km and 5 km, respectively. Forty-five vertical levels are used in each domain with a higher resolution in the planetary boundary layer.[1]

Model configurations for the eighteen ensemble members in the WRF and MM5 models are given in Table 1. The perturbed initial conditions (ICs) include variations in the atmospheric first-guess states (partial cycle or cold start), data assimilation with or without bogus observations, and one-way or two-way interactive nesting schemes among multiple domains. While a two-way interaction approach with a storm-following nest would function better for typhoon forecasting (Fang and Zhang, 2012), the this study focused on investigating typhoon rainfall over a mountainous watershed with the operational ensemble forecast technique. Thus, a two-way interactive nesting scheme with a storm-following nest is beyond the scope of this study.

Cold start runs were initialized with large-scale fields that were obtained from the NCEP Global Forecast System (GFS) analyses. Partial cycle runs included a cold start 12 h before the analysis time

---

[1] The vertical 45-level eta (sigma for MM5) values in the terrain-following coordinate are 1.0, 0.995, 0.988, 0.98, 0.97, 0.96, 0.945, 0.93, 0.91, 0.89, 0.87, 0.85, 0.82, 0.79, 0.76, 0.73, 0.69, 0.65, 0.61, 0.57, 0.53, 0.49, 0.45, 0.41, 0.37, 0.34, 0.31, 0.28, 0.26, 0.24, 0.22, 0.2, 0.18, 0.16, 0.14, 0.12, 0.1, 0.082, 0.066, 0.052, 0.04, 0.03, 0.02, 0.01 and 0.0.

and then two 6-h data assimilation cycles. In addition, two statistical background error covariance matrices (CV3 and CV5) and the outer loop (OL) procedure in the three-dimensional variational data assimilation system (3DVAR; Skamarock et al., 2008) were also included as initial-condition perturbations. Furthermore, a four-dimensional variational data assimilation system (4DVAR) and a no-data-assimilation (NODA) run were included in the MM5 model configuration. Dynamically consistent bogus vortices were imposed near the observed typhoon position for most of the 3DVAR or 4DVAR analyses (Park and Zou, 2004; Hsiao et al., 2010). Lateral boundary conditions (LBCs) were provided every 6 h from the NCEP global forecast system, except that ensemble member 12 has LBCs from the Taiwan Central Weather Bureau (CWB) global model.

Variations in cumulus schemes included the Grell–Devenyi ensemble (GD; Grell and Devenyi, 2002), Grell 3D ensemble (G3; Grell and Devenyi, 2002), Betts–Miller–Janjic (BMJ; Betts et al., 1986; Janjic, 1994), Kain–Fritsch (KF; Kain and Fritsch, 1990), and Grell scheme (Grell, 1993; used only for MM5). These cumulus parameterization schemes were used in Domains 1 and 2 (with grid sizes of 45 and 15 km). Only the microphysics scheme was used in Domain 3 because a grid size of 5 km can resolve convection explicitly. Preliminary experiments in 2010 indicated that these various cumulus scheme variations effectively provided physical perturbations in this ensemble model configuration (not shown). Microphysics schemes included the Goddard (Tao et al., 2003) and WRF Single-Moment 5-class scheme (WSM5; Hong et al., 2004), and the same microphysics scheme was used in three nested domains. Planetary boundary layer schemes included the Yonsei University scheme (YSU; Hong et al., 2006) and the medium-range forecast (MRF) nonlocal boundary layer scheme (Hong and Pan, 1996). The ensemble forecasting system included 18 members and was run operationally four times a day (initialized at 0000 UTC, 0600 UTC, 1200 UTC, and 1800 UTC) at the Taiwan Typhoon and Flood Research Institute (TTFRI). This forecasting system produced the 72-h track and rainfall forecasts for invading typhoons in 2011.

Because the accuracy of forecasting rainfall forecast in Taiwan watershed depends on the track forecasts, the ensemble forecasts were first evaluated for track prediction. Torn and Davis (2012) identified track-error differences of up to 25% for different cumulus schemes in their 36-km WRF model. A similar sensitivity to cumulus schemes was found in a preliminary study for typhoons in 2010 (not shown). In contrast, additional variations beyond the Goddard microphysics and YSU PBL schemes with this ensemble model configuration did not generate noticeable differences in typhoon track forecasts in 2010. Therefore, the key physical perturbations in the WRF model resulted from the five cumulus schemes in the ensemble configuration.

2.2.3. Hydrological model: WASH123D

The physically distributed hydrological model was the WAterSHed Systems of the 1-D Stream-River Network, the 2-D Overland Regime, and the 3-D Subsurface Media (WASH123D) model. The WASH123D model was first developed by Yeh et al. (1998) and was later modified to increase its capability and flexibility. The WASH123D model has been applied in over 60 research projects around the world. For example, it was chosen by the U.S. Army Corps as the core computational code for modeling the Lower East Coast (LEC) Wetland Watershed and was used to construct a Regional Engineering Model for Ecosystem Restoration (REMER). In addition, the use of a revamped WASH123D model was proposed for disaster reduction to predict flood and inundation in several Taiwan river basins (Yeh et al., 2011).

In this model, the finite-element approach was used to represent the hydrological processes at various spatial and temporal
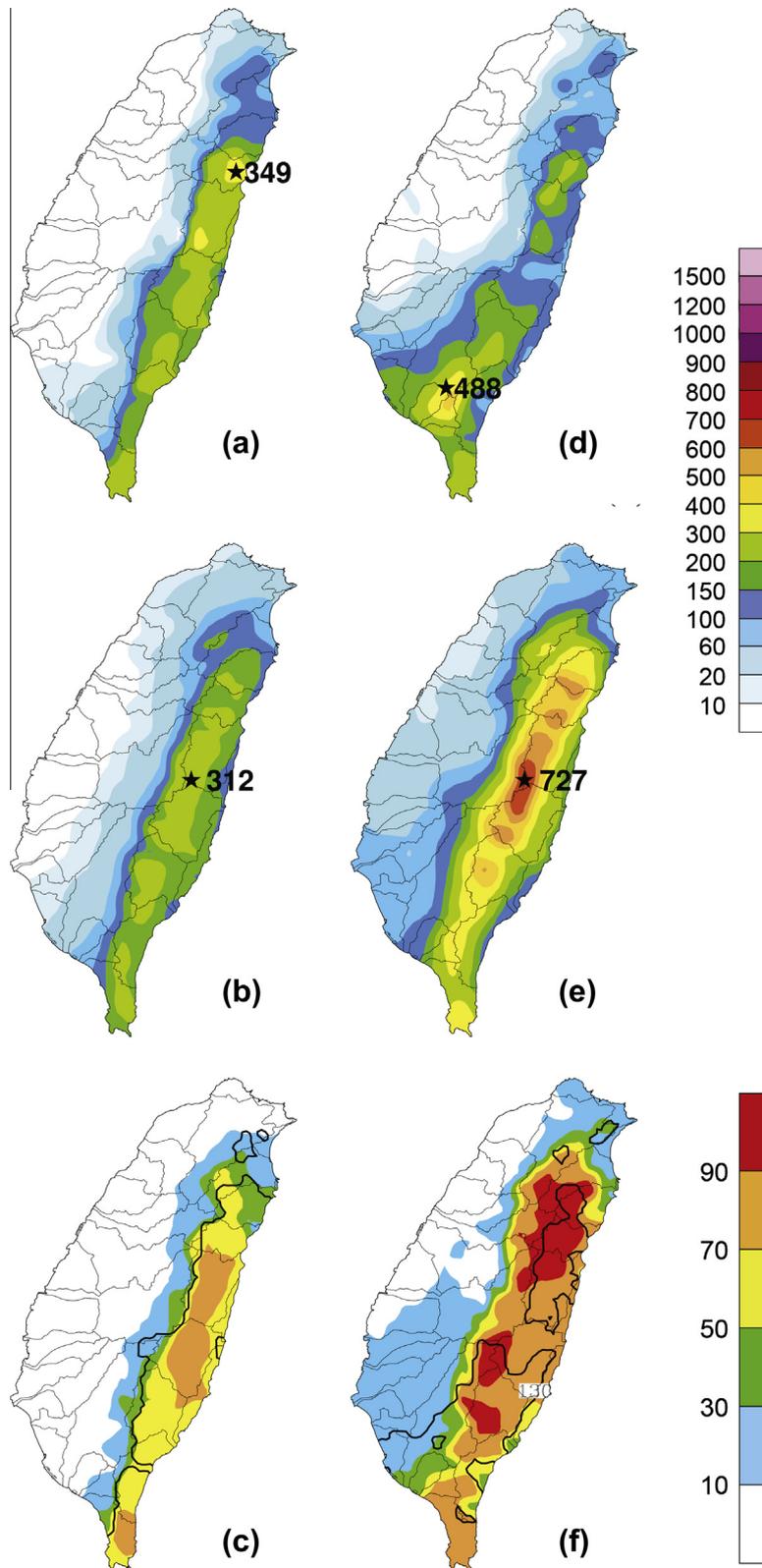
Fig. 7. The 0–24-h accumulated rainfall from the forecast initiated at 1200 UTC 27 August: (a) observed rainfall, (b) ensemble mean from 18 members, and (c) the rainfall probability distribution (%) exceeding the threshold of 130 mm for 18 ensemble members. The observed rainfall at the 130-mm threshold is shown by the black solid lines. (d, e, and f) as in panels (a, b, and c), except for the 24–48-h accumulated rainfall.

scales. The terrain spatial resolution of the WASH123D model was 400 m by 400 m in the Lanyang mountainous areas. Finer grids of 40 m by 40 m were applied near the river/overland boundaries. The inner 5-km rainfall from the atmospheric model was interpo-

lated to the WASH123D model terrain using nearest neighbor interpolation. The flows in the watershed system, which used the river and overland diffusive wave equations, were solved with the semi-Lagrangian and Galerkin finite-element methods to
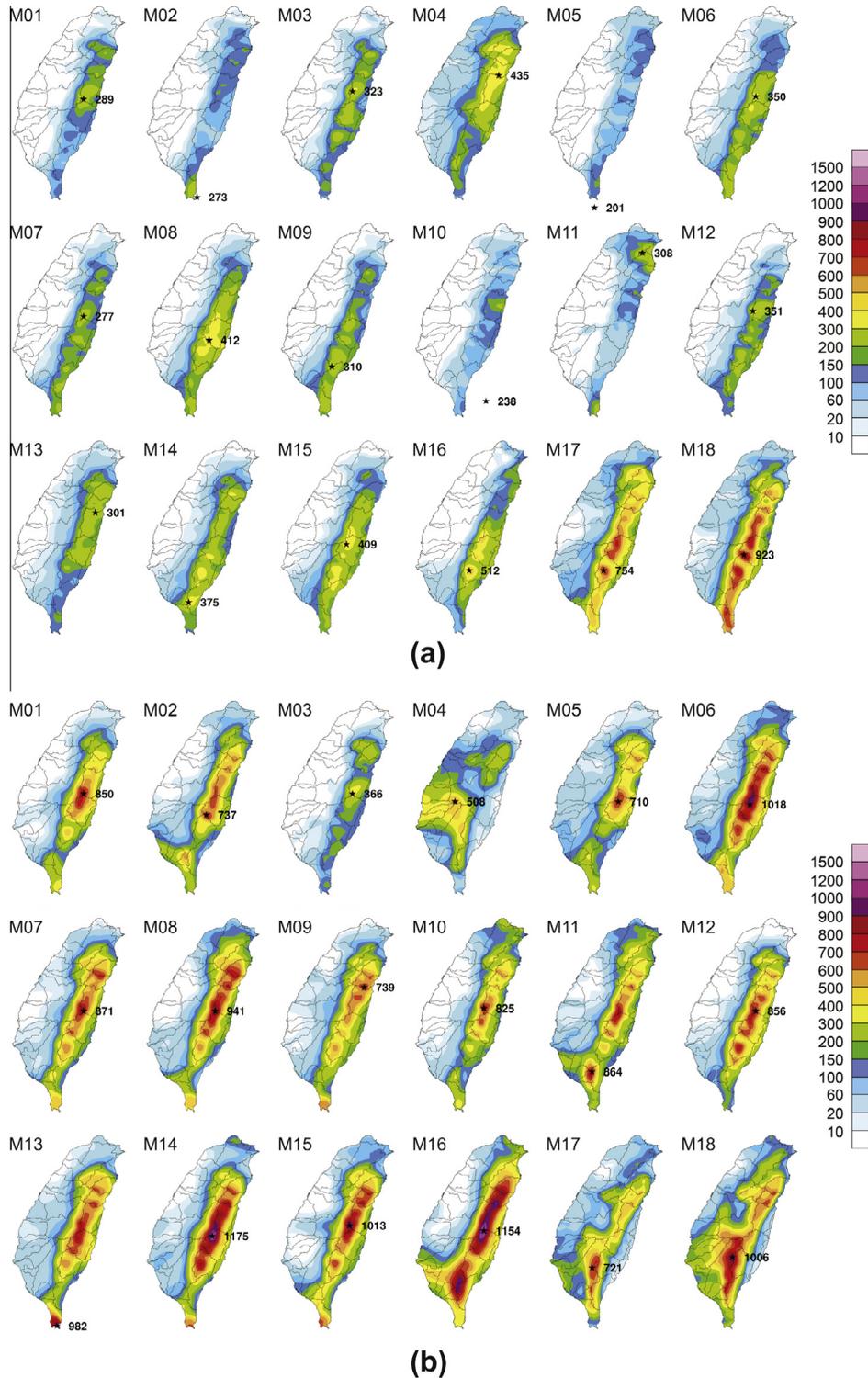
Fig. 8. Spatial distribution of (a) the 0–24-h and (b) the 24–48-h accumulated rainfall forecast (mm) at 1200 UTC 27 August over Taiwan for the 18 ensemble members.

determine the coastal inundations. Initial conditions were obtained from measurements or from steady-state simulations of the governing diffusive wave equations.

2.3. Skill score descriptions

In Section 4, the threat score (TS), equitable threat score (ETS), bias score (BS), and false alarm rate (FAR) are presented for the 5-km grid rainfall forecasts for Typhoon Nanmadol between 1200

UTC 27 August and 0000 UTC 30 August 2011. The TS is defined as follows:

$$TS = \frac{H}{F + O - H},$$
(1)

where H is the number of hits, and F and O are the numbers of points in which the forecast or observed rainfall amounts are greater than the specified threshold. The ETS is equivalent to the TS
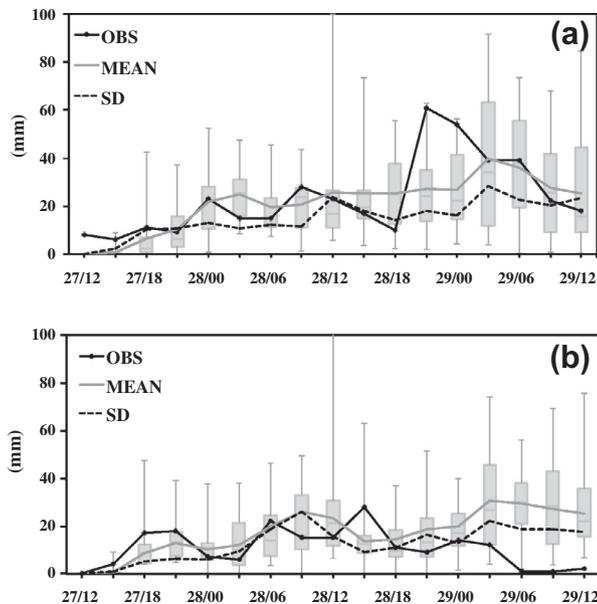
Fig. 9. Time series of areal-average 3-h rainfall (in units of mm) for (a) three basins over southern Taiwan and (b) Lanyang basin from the ensemble members with minimum, lower quartile, median, upper quartile, and maximum depicted by box-and-whiskers plot from the forecast initiated at 1200 UTC 27 August, and the ensemble mean (MEAN; gray solid line), the rainfall observations (OBS; black solid line), and standard deviation (SD; black dash line).

except after the removal of those hits that are attributed to random guesses. The ETS is defined as follows:

$$\text{ETS} = \frac{H - R}{F + O - H - R}, \tag{2}$$

where R is the number of hits from random guesses (with $R = FO/N$), and N is the total number of points that are being verified. The BS is defined as the ratio of the number of forecasted points to the number of the observed points in which the rainfall is above a specified threshold ($BS = F/O$). In addition, the FAR is the ratio of the unsuccessful forecasts to the total number of forecasts [FAR = $(F - H)/F$]. The rainfall threshold used in this study is 130 mm per day, which is defined as *torrential rainfall* by the CWB.

The standard deviations (SD) of the rainfall among the ensemble members are used to quantify the variability in the ensemble forecast. The SD is defined as follows:

$$\text{SD} = \sqrt{\frac{1}{M} \sum_{m=1}^{M} [R_m(i,j,t) - \bar{R}(i,j,t)]^2} \tag{3}$$

where m denotes the ensemble member index, M is the number of ensemble members (18), R_m is the individual forecast, $\bar{R}$ is the ensemble mean, i and j are the horizontal gridpoint indices, and t is the time.

3. Track verifications

To establish the veracity of the track forecast ensemble system, 219 forecasts from 21 typhoons in 2011 were verified relative to the observed (CWB best-track analysis) TC positions (Fig. 4). In general, the ensemble mean forecast was more accurate than the individual ensemble member forecast, particularly before the first 24 h. The ensemble mean track errors for the 21 typhoons were 93, 180, 295 km at 24, 48, and 72 h forecasts, respectively. These track error values were superior to the Navy Operational Global Atmospheric Prediction System (NOGAPS) values of 140, 216, and

316 km. Thus, the ensemble forecast system that was used in this study is capable of producing accurate typhoon track forecasts that are necessary for rainfall forecasts.

The ensemble-mean track errors were 59, 91, and 229 km for the 24, 48, and 72 h track forecasts of the 11 forecasts for Typhoon Nanmadol (Fig. 4), respectively. Because the ensemble track forecasts of Nanmadol were better than the average for the 21 typhoons in 2011, it was expected that the ensemble would produce a better rainfall forecast. In the next section, these ensemble rainfall forecasts for Typhoon Nanmadol and the flood simulations from the WASH123D hydrological model are evaluated.

4. Rainfall verification

The TS, BS, ETS, and FAR which are calculated for the 18 individual members and the ensemble mean from rain gauge data over Taiwan with the Kriging technique when the daily rainfall exceeded 130 mm (Fig. 5). The ensemble mean rainfalls had TSs that exceeded 0.4, except for the forecast initialized at 0000 UTC 30 August (when Nanmadol was rapidly weakening). As expected, the ensemble mean was always better at forecasting rainfall (in terms of TS) than the individual members. Recall that a BS of 1 indicates a perfect forecast, a BS < 1 indicates under-forecasting, and a BS > 1 indicates over-forecasting. In general, the BS increased as Nanmadol approached Taiwan and made landfall at 1800 UTC 28 August and then quickly decreased after landfall (Fig. 5b). Thus, the ensemble rainfall forecasts tend to be over-forecasting. This over-forecasting tendency is attributed to the systematic over-prediction of windward rainfall, which is associated with typhoon circulation impinging on the Taiwan terrain. Yang et al. (2008; their Figs. 6 and 7), Chien et al. (2002; their Fig. 9), and Yang et al. (2004; their Fig. 6) found similar rainfall over-forecasting in the mountainous regions of Taiwan during the typhoon and Mei-Yu seasons.

When Typhoon Nanmadol was far from Taiwan and the rainfall reduced after 0000 UTC 29 August, lower ensemble mean values were generally associated with higher TS values. This may be explained by the reduced FAR during this period (Schaefer, 1990). The FAR was reduced and the BS decreased after 0000 UTC 29 August, when the extreme rainfall was gradually mitigated (Fig. 5d). Meanwhile, the ensemble mean had a lower false alarm rate (FAR) and a higher hit rate (ETS) than the individual members.

Similarly, the ETS indicates the best rainfall forecast skill for the ensemble mean. As expected, these ETS scores are less than the TS because of the removal of hits from the random guesses. Furthermore, the ETS variability among the ensemble members was similar to that of the TS. Overall, the forecast uncertainties that were reflected in these scores became large, when Typhoon Nanmadol was far away from Taiwan and when it started to weaken. The greater rainfall uncertainties that occurred when Nanmadol was far from Taiwan might result from larger track errors and the lack of the observations over the ocean. In the later stage, the weakened Nanmadol circulation was phase-locked to the topography, which would result in greater uncertainty.

To examine the improvements in the ensemble rainfall forecasts and runoff simulations, two cases for the forecasts that were initiated at 1200 UTC 27 August and at 1200 UTC 28 August (Fig. 6) were selected. These forecasts contained large and small rainfall variabilities that likely result from large and small typhoon track forecasts variabilities, respectively. In the ensemble forecast initialized at 1200 UTC 27 August, the TC positions of all ensemble members are to the east of the observed TC center (Fig. 6a). Translation was slow as the TC was forecasted to approach Taiwan (Fig. 6a). In this stage, large track errors occurred because
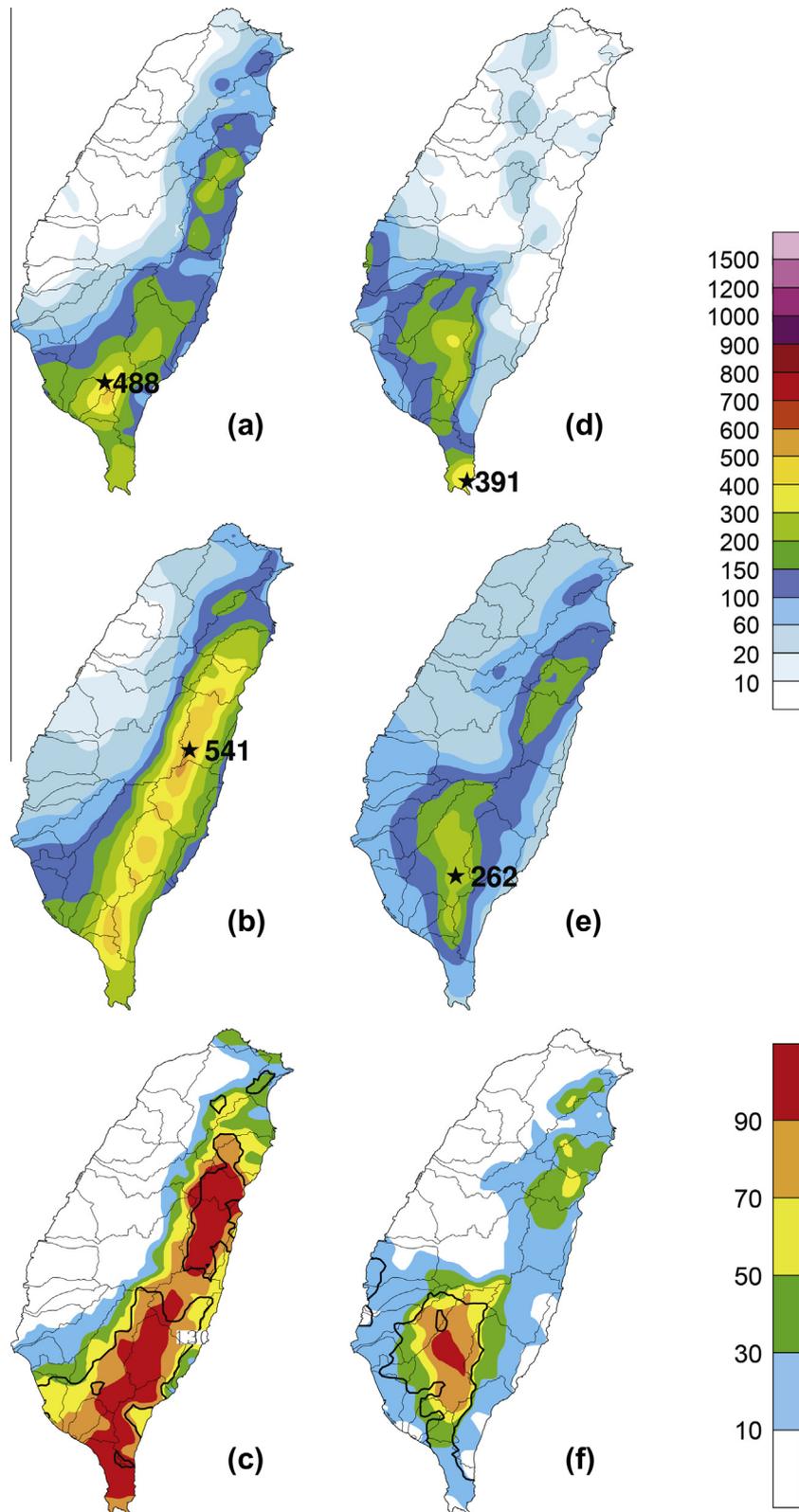
Fig. 10. As in Fig. 7, except from the forecast initiated at 1200 UTC 28 August.

Nanmadol had passed Taiwan. A slow translation can enhance rainfall over Taiwan (e.g. Typhoon Morakot, Chien and Kuo, 2011). For example, the forecasted rainfall (Fig. 7e) was much greater than the observed (Fig. 7d) for the 24–48 h period. How-ever, the accumulated rainfall during the first 24 h was similar

between the observed (Fig. 7a) and the forecasted rainfall when the track errors were smaller.

The 18 individual ensemble members for the 0–24 h accumu-lated rainfall forecasts are provided in Fig. 8a. In these ensemble forecasts, the maximum 24-h rainfall occurs over eastern Taiwan,
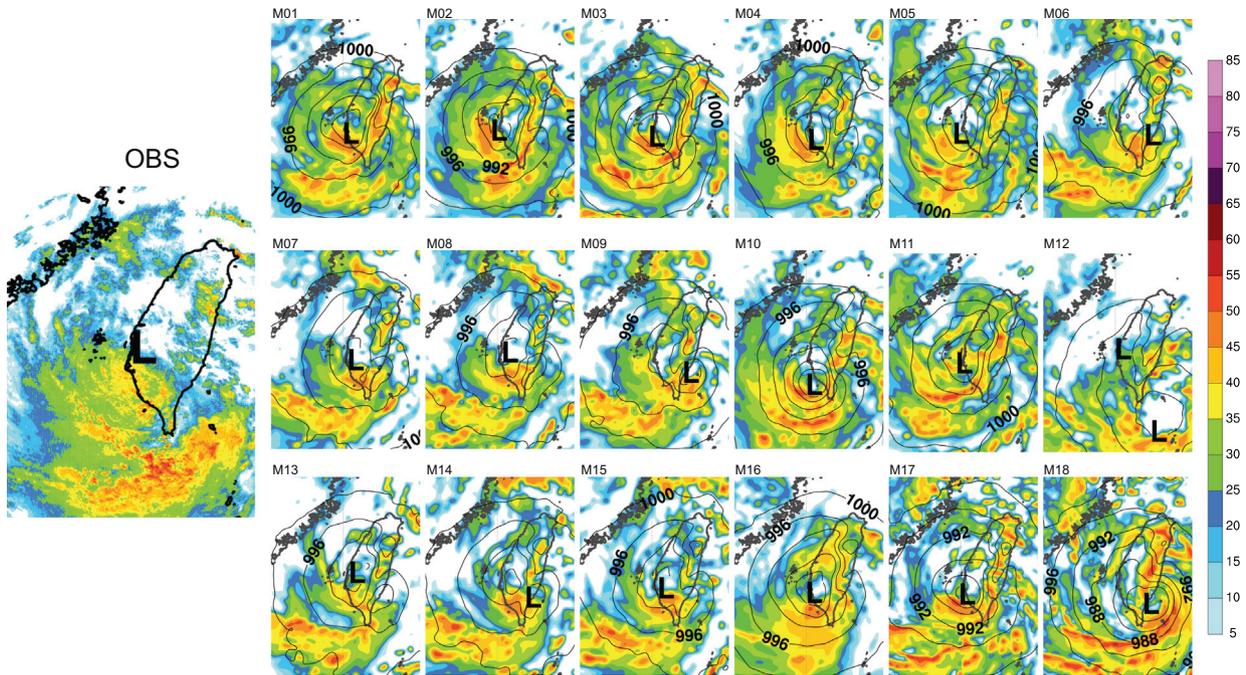
Fig. 11. Spatial distribution of radar reflectivity (dBZ) from observations (OBS) at 0000 UTC 29 August (left panel) for the 18 ensemble members (right panels) at 12 h in the forecast initiated at 1200 UTC 28 August.

except for the M02 and M05 members. The forecast tracks for these two members were two outliers (Fig. 6a). Thus, the typhoon-topography interactions (and the associated rainfall features) were not properly captured. The two MM5 ensemble members (M17 and M18) predicted that more rainfall would occur in eastern Taiwan than the two members (M14 and M15) that were based on the WRF model with similar 0–24 h forecast tracks. This early rainfall forecast from the two MM5 members resulted from a more rapid translation speed. Thus, the interaction between the typhoon circulation and the Central Mountain Range occurred earlier.

Regarding the 24–48 h forecasts (Fig. 8b), the slow movement of the ensemble TCs (Fig. 7e) contributed to the accumulation of rainfall, which significantly increased over the eastern CMR. Although the maximum 24–48 h accumulated rainfall that resulted from Typhoon Nanmadol was 488 mm in Pingtung County (Fig. 7d), the rainfall distributions from the ensemble members indicated over-forecasting in eastern Taiwan. This over-forecasting
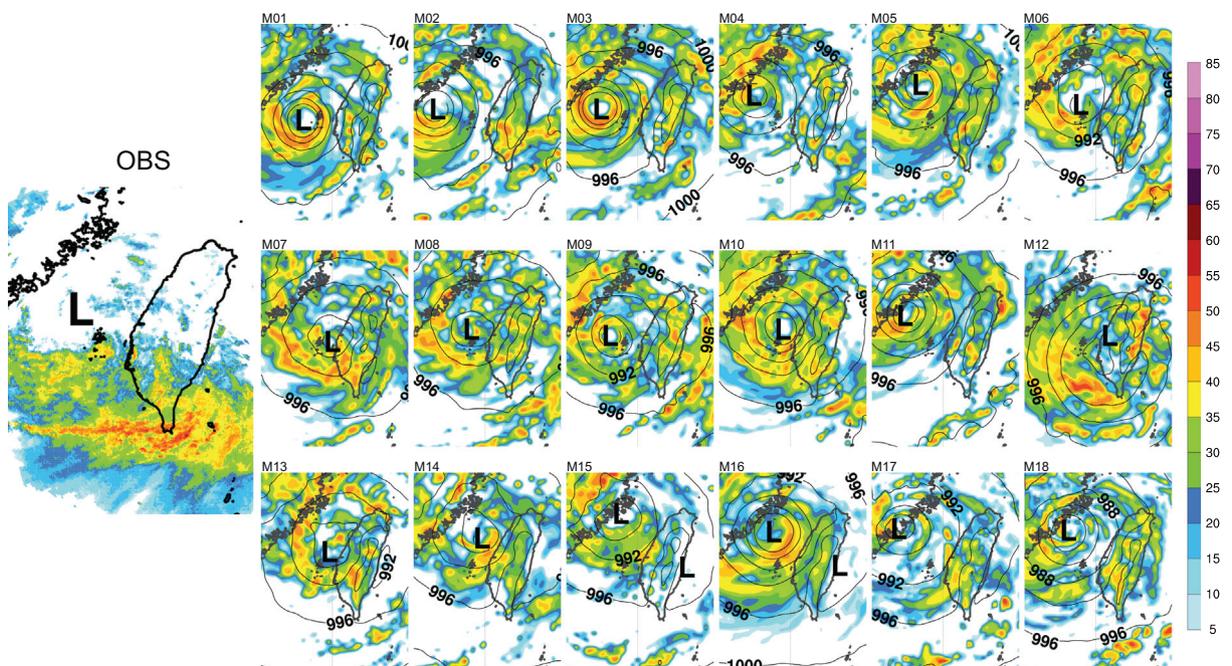

Fig. 12. As in Fig. 11, except for the observations (OBS) at 0000 UTC 30 August (left panel) and for the 18 ensemble members at 36 h in the forecast initiated at 1200 UTC 28 August.
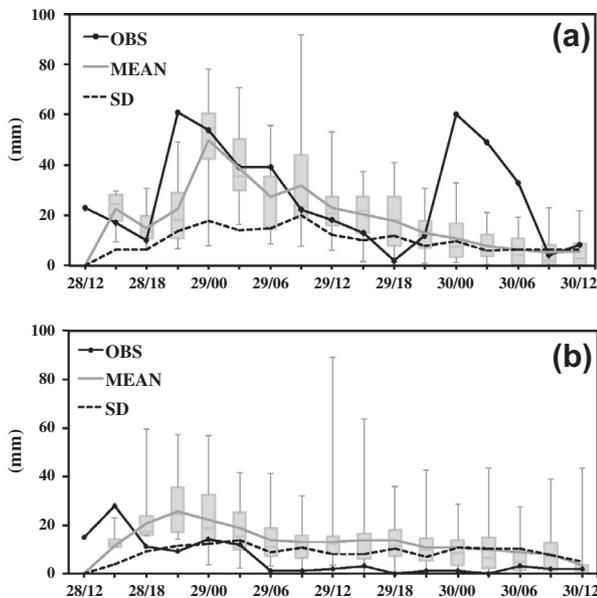
Fig. 13. As in Fig. 9, except for the ensemble forecast initiated at 1200 UTC 28 August.
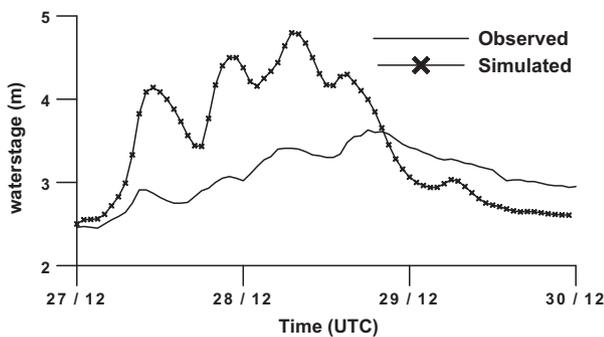

Fig. 14. Comparison of water stages (m) between the measurements and the WASH123D simulation driven by rain gauge observations starting from 1200 UTC 27 August.

resulted from the interaction of the CMR with the under-forecasting in southern Taiwan (Fig. 8b). These ensemble rainfall forecasts illustrate phase locking with the CMR and the importance of accurate path and translation speed forecasts.

Based on these rainfall forecasts from the ensemble modeling system, the rainfall probability distributions for the 24-h threshold of 130 mm in the two forecast periods are shown in Fig. 7c and f. The 130-mm observed rainfall thresholds (black solid lines in Fig. 7c and f) occurred in eastern Taiwan during the 0–24 h forecast, and in eastern and southern Taiwan during the 24–48 h forecast. Between 50% and 90% of the ensemble members predicted a 0–24 h rainfall of more than 130 mm in eastern Taiwan (Fig. 7c). In comparison, a more than 70% probability for rainfall above 130 mm for the 24–48 h forecast was predicted for eastern Taiwan and only a 30–70% probability of rainfall above 130 mm was found for southern Taiwan (Fig. 7f). This accurate torrential rainfall probability information would be very useful for guiding forecast and planning hazard mitigation operations. Additional evaluations that contain this type of probability information from ensemble predictions are recommended.

Time series of the areal-average 3-h rainfall for the three basins (Nanping-Donghe, Tungkang, and Linpien river basins; see Fig. 2) with maximum rainfall in southern Taiwan are shown in Fig. 9. In general, the comparison of the time series of the standard deviations (SD; dash line) and ensemble means (MEAN; gray solid line) in Fig. 9 indicates that the SD and MEAN values are in phase. Thus, the larger the ensemble mean, the larger the forecast variability [also see Fig. 5 of Fang et al. (2011)]. For the three southern basins (Fig. 9a), the ensemble mean rainfall forecast was generally consistent with the observed rainfall except for the period between 1800 UTC 28 August and 0300 UTC 29 August, and in eastern Taiwan for the 0–24 h forecast (as shown in Fig. 9b). Similarly, the basin rainfall indicated under-forecasting over the southern basin and over-forecasting over the eastern basin for the 24–48 h forecast.

The rainfall distributions from the forecast that were initiated at 1200 UTC 28 August (Fig. 10) had smaller TS variability (Fig. 5a), which was attributed to the accurate track forecasts because the ensemble mean track errors were only 12 and 52 km for the 24 h and 48 h forecasts, respectively (Fig. 6b). Nevertheless, when the 0–24 h and 24–48 h accumulated rainfall predictions (Fig. 10b and e) were compared with the observations (Fig. 10a and d), both predictions accurately forecasted the rainfall distribution over the eastern CMR but over-forecasted the maximum rainfall amounts.

The ensemble mean rainfall forecast did not accurately predict the distribution of rainfall over southern Taiwan during the 24–48 h forecast period (Fig. 10e). The rainfall probability distribution for the torrential-rainfall threshold of 130 mm from the ensemble forecast initiated at 1200 UTC 28 August indicated more than 90% probability of the heavy rainfall over the eastern and southern Taiwan during the 0–24 h period (Fig. 10c). However, the probability distribution of the heavy rainfall was maximized of 90% over a small area in southern Taiwan during the 24–48 h forecast period (Fig. 10f).

Simulated radar reflectivity values at 12 h in the forecast initiated at 1200 UTC 28 August for each ensemble member indicated that a stronger radar echo (compared to the observed echo) was predicted in the northeast quadrant of Nanmadol (Fig. 11). This is consistent with the systematical over-prediction of windward precipitation over the CMR for the 18 ensemble members (especially for the MM5 members M17 and M18; see Fig. 11). In addition, similar excessive radar echoes are forecasted along the eastern CMR at 36 h (Fig. 12). A narrow, east–west oriented rainband in the observed radar reflectivity likely contributed to a maximum in precipitation near the southern tip of Taiwan (see Fig. 10d). Such a narrow band cannot be predicted accurately with the current ensemble model, which has a horizontal grid size of 5 km on the innermost grid.

The time series for the areal-average 3-h rainfall in the three southern basins based on ensemble forecasting (beginning at 1200 UTC 28 August) are provided in Fig. 13a. Two rainfall maxima were associated with typhoon-induced deep convection, which occurred around 2100 UTC 28 August and at 0000 UTC 30 August (after Nanmadol had passed over Taiwan). Although the ensemble mean forecast can reasonably predict the first maximum, it is unable to predict the second rainfall maximum. The relationship between the ensemble mean rainfall and the SD of the rainfall among the ensemble members was somewhat weaker than that shown in Fig. 9. Thus, these results were not consistent with the rainfall observations. For the Lanyang basin (Fig. 13b), a single rainfall maximum was observed early in the forecast period that was initiated at 1200 UTC 28 August. Although the ensemble mean forecast had a similar rainfall maximum, it was delayed by 6 h. In general, the ensemble forecasted two large 3-h rainfall events during the 48 h period and after 0300 UTC 29 August, when very small amounts of rainfall were observed over the Lanyang basin.
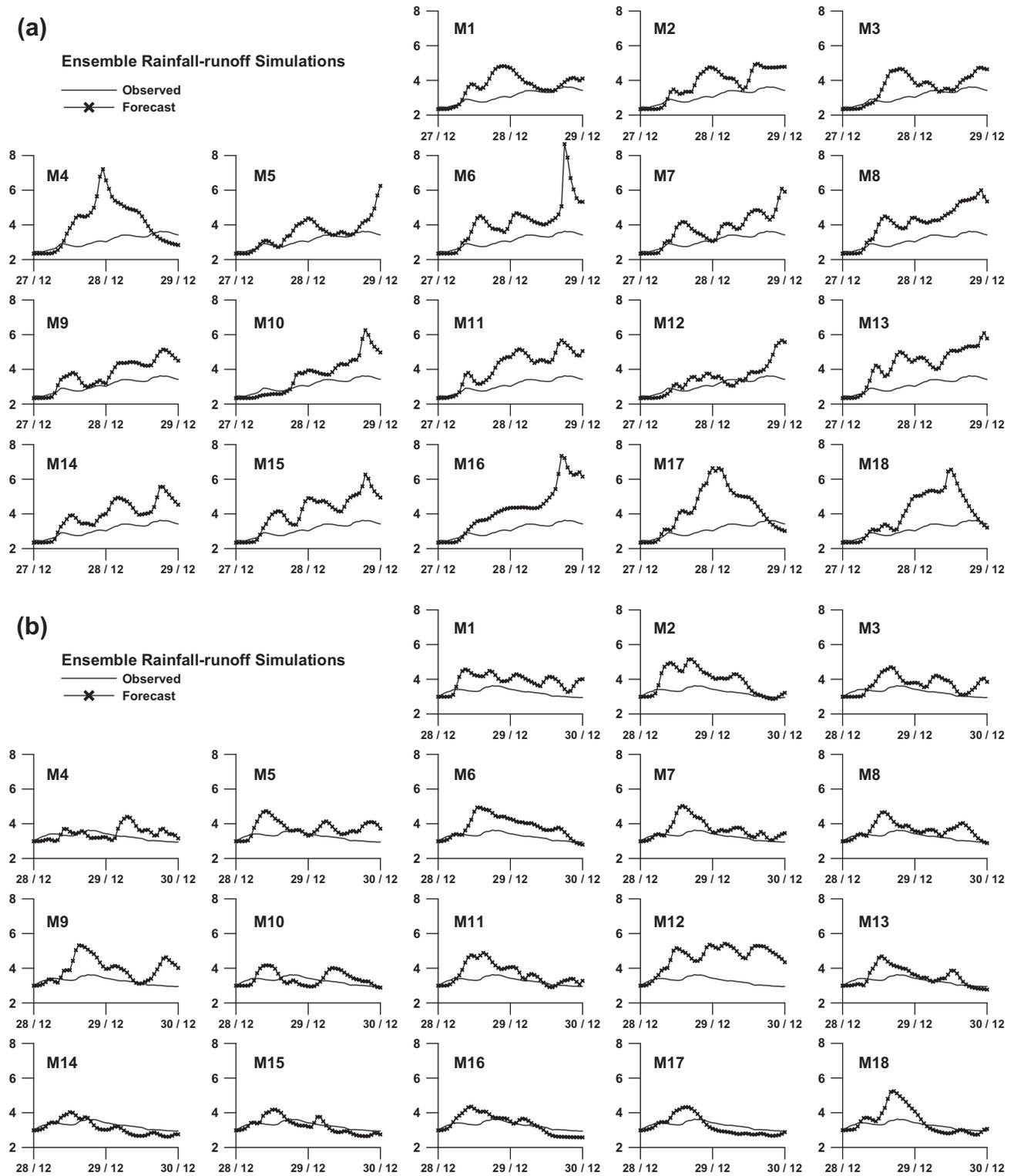
Fig. 15. As in Fig. 14, except for the 48-h simulation driven by 18 ensemble member rainfall amounts starting at (a) 1200 UTC 27 and (b) 1200 UTC 28 August.

5. Hydrological verification

First, the observed water stages at the two sites in Fig. 2 (insert) were compared with the water stages from the WASH123D hydrological model, which was driven by the 17 rain gauge observations. Details regarding the parametric assessment and the identification of the distinctive model coefficient ranges are given in Shih and Yeh (2011). The measured water stage at 1200 UTC 27 August was used as an initial condition for the WASH123D watershed simulation (Fig. 14). The observed water stage gradually increased. However, the simulated hydrograph over-predicted the water stage until approximately 1200 UTC 29 August. Next, the water stage was under-predicted.

An integrated watershed simulation that includes groundwater calculations for flood forecasting has not been considered as a practical alternative in Taiwan due to its steep terrain and the
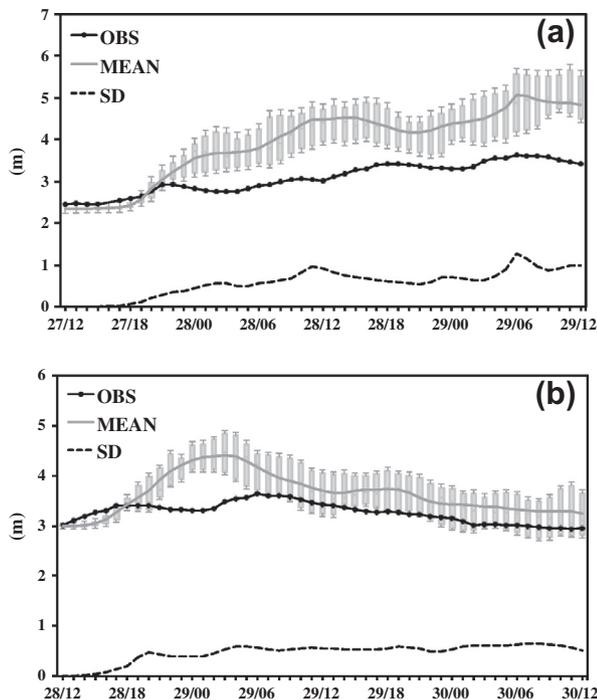
Fig. 16. Hourly time series of the areal-averaged water stage (in units of m) for the Lanyang basin estimated from the ensemble members with minimum, lower quartile, median, upper quartile, and maximum depicted by box-and-whiskers plots for the ensemble forecasts initiated at (a) 1200 UTC 27 August and (b) 1200 UTC 28 August, and hourly water stage from ensemble mean (MEAN; gray solid line), the observation (OBS; black closed circles), and standard deviation (SD; black dash line).

resulting short hydraulic response times. Therefore, groundwater routing was ignored in this WASH123D hydrological model.

Thus, surface routing with the coupled river/overland simulation for rainfall–runoff prediction was used to facilitate efficient modeling. Next, an infiltration mechanism (i.e., Green–Ampt model) was applied to evaluate the effective rainfall. Therefore, it became important to obtain an appropriate effective rainfall distribution for driving the runoff simulation. The runoff simulation generally performed better during extreme flooding events, in which water storage in the river channel varies rapidly, than under gentle hydrography. During Typhoon Nanmadol, most of the rainwater was presumed to have infiltrated into the groundwater. Thus, excess overland flow was assumed to move slowly due to the dry soil conditions. This gradually increasing hydrograph behavior (as shown in the observed curve in Fig. 14) may not be captured by the present version of the WASH123D watershed model, which does not consider groundwater routing.

To establish a prototype hydrological model for the real-time operational flood warning system, the ensemble rainfall forecasts were used to drive a watershed model for runoff simulation. Runoff from the Lanyang basin was simulated for each member by using the WRF/MM5-WASH123D integrated modeling system (Fig. 15). Each simulated hydrograph from the WASH123D model was driven by a rainfall forecast from the WRF/MM5 model. In the simulation from 1200 UTC 27 August to 1200 UTC 29 August (Fig. 15a), the water stage was over-predicted by the ensemble members. The simulation from 1200 UTC 28 August to 1200 UTC 30 August (Fig. 15b) indicated a water stage maximum at approximately 1200 UTC 29 August. In this case, most of the simulated water stages were lower and were closer to the observed water stages.

The water stage runoff simulations for mountainous watersheds are highly sensitive to the rainfall time series prediction (Fig. 16). Just as the WASH123D model over-predicted the water

stage when driven by the rain gauge data, river runoff was over-forecasted when driven by the ensemble rainfall forecast. When the river water stage was high, more precipitation directly affects rainfall because the soil is moist. In general, this integrated hydrometeorology modeling system is useful for predicting (albeit a likely over-forecast) the occurrence of extreme floods during typhoon events in the mountainous watersheds on the windward side of Taiwan. This result can be used in other mountainous watersheds by using hydrological models that are familiar based on local soil conditions.

6. Conclusions

An ensemble WRF/MM5 forecasting system for predicting typhoon-related rainfall and a physically distributed hydrological model (WASH123D) were one-way coupled to forecast flooding during the landfall of Typhoon Nanmadol (2011). This is the first attempt to use a coupled ensemble-hydrometeorological method over mountainous watersheds in Taiwan. This ensemble configuration provided a better track prediction than the deterministic prediction model for 219 cases that involved 21 typhoons in 2011. Because the ensemble mean track forecasts are similar to other operational centers, it was hypothesized that the ensemble tracks would be useful for providing a time series of rainfall estimates when a typhoon approaches a mountainous watershed. While the spatial pattern and the amount of accumulated rainfall depend on the typhoon track and on the effects of Taiwan's mountainous terrain on typhoon circulation, a high-resolution ensemble model is required to predict fine-scale spatial and temporal characteristics of convective rainfall features

For Typhoon Nanmadol, the rainfall along the eastern CMR was consistently over-forecasted by the ensemble modeling system due to the over-enhancement of windward precipitation by the Taiwan topography. However, the track of the typhoon was almost perfectly forecasted. In addition, the ensemble modeling system provided useful probabilistic rainfall information. For example, the 90% probability that the accumulated rainfall exceeded 130 mm for the 0–24 h forecast that was initiated at 1200 UTC 28 August, which corresponded well with the observed distribution of the 130 mm of rainfall. The standard deviations of the rainfall that was derived from the ensemble prediction system were generally consistent with the timing of the heavy rainfall events. Furthermore, the ensemble forecasting system adequately estimated the topographic locations where rainfall may occur.

A watershed model that was driven by the amount of ensemble forecasted rainfall was tested for Lanyang basin during Typhoon Nanmadol. If water stage measurements are provided to serve as the initial values for watershed modeling, the ensemble member rainfall forecasts can be used as inputs in the watershed model. In this case, the river runoff patterns were reasonably predicted despite the mismatch between the runoff maximum and the actual time and quantity of flooding. The ensemble rainfall standard deviation provides useful information regarding the probability of a flood event. Due to the systematic over-prediction of windward basin precipitation by the ensemble model, the simulated hydrograph over the Lanyang watershed was also over-forecasted. In addition, the omission of a ground water routing component in the watershed model contributed to the over-prediction of river runoff. Thus, despite adequate forecasting of typhoon-induced rainfall on the island, additional research is required to provide detailed temporal and spatial flooding distributions for watersheds with complex terrain. In addition, the infiltration calculation should be further improved to accurately model infiltration in very dry soils and effective typhoon rainfall in the future.

The prediction of flooding downstream of a mountainous watershed is highly sensitive to rainfall predictions. The hydrology

model that is one-way-coupled with the ensemble meteorological forecasts provides useful probability information for the runoff forecasting. Despite the systematic over-prediction of rainfall and water stage in the watershed on the windward side of Taiwan, the coupled hydrometeorological modeling system can potentially improve the accuracy and timing of flood predictions during the approach of a typhoon.

Acknowledgments

References

Betts, A.K., Miller, M.J., 1986. A new convective adjustment scheme. Part II: Single column tests using GATE wave, BOMEX, and arctic air-mass data sets. Quart. J. Roy. Meteor. Soc. 112, 693–709.

Bowler, N.E., Arribas, A., Mylne, K.R., Robertson, K.B., Beare, S.E., 2008. The MOGREPS short-range ensemble prediction system. Quart. J. Roy. Meteor. Soc. 134, 703–722.

Bras, R.L., Rodriguez-Iturbe, I., 1985. In: Random Functions and Hydrology. Addison-Wesley, Reading, p. 559p.

Buizza, R., 2007. The new ECMWF variable resolution ensemble prediction system. Thielen, J., Batholmes, J., Schaake, J. (Eds.), Book of Abstracts of the 3rd HEPEX Workshop, Stresa, Italy, European Commission EUR22861EN, 27–29 June, 2007, pp. 19–23.

Chien, F.C., Kuo, H.C., 2011. On the extreme rainfall of typhoon Morakot (2009). J. Geophys. Res. 116, D05104. http://dx.doi.org/10.1029/2010JD015092.

Chien, F.C., Kuo, Y.H., Yang, M.J., 2002. Precipitation forecasts of the MM5 in Taiwan area during the 1998 Mei-Yu season. Weather Forecast. 17, 739–754.

Clark, A.J., Gallus, W.A., Xue, M., Kong, F., 2010. Convection-allowing and convection-parameterizing ensemble forecasts of a mesoscale convective vortex and associated severe weather environment. Weather Forecast. 25, 1052–1081.

Du, J., DiMego, G., Toth, Z., Jovic, D., Zhou, B., Zhu, J., Chuang, H., Wang, J., Juang, H., Rogers, E., Lin, Y., 2009. NCEP short-range ensemble forecast (SREF) system upgrade in 2009. In: 19th Conf. on Numerical Weather Prediction and 23rd Conf. on Weather Analysis and Forecasting, Omaha, Nebraska, Amer. Meteor. Soc., June 1–5, 2009, 4A.4.

Epstein, E.S., 1969. The role of initial uncertainties in prediction. J. Appl. Meteor. 8, 190–198.

Fang, J., Zhang, F., 2012. Effect of beta shear on simulated tropical cyclones. Mon. Weather Rev. 140, 3327–3633.

Fang, X., Kuo, Y.-H., Wang, A., 2011. The impacts of Taiwan topography on the predictability of Typhoon Morakot's record-breaking rainfall: a high-resolution ensemble simulation. Weather Forecast. 26, 613–633.

Grell, G.A., 1993. Prognostic evaluation of assumptions used by cumulus parameterizations. Mon. Weather Rev. 121, 764–787.

Grell, G.A., Devenyi, D., 2002. A generalized approach to parameterizing convection combining ensemble and data assimilation techniques. Geophys. Res. Lett. 29 (14). Article 1693.

Grell, G.A., Dudhia, J., Stauffer, 1995. A Rete/NCAR Mesoscale Model (MM5). NCAR Tech. Note NCAR/TN-398 STR, 122p.

Hamill, T.M., Whitaker, J.S., Fiorino, M., Benjamin, S.G., 2011. Global ensemble predictions of 2009's tropical cyclones initialized with an ensemble Kalman filter. Mon. Weather Rev. 139, 668–688.

Hong, S.-Y., Pan, H.-L., 1996. Nonlocal boundary layer vertical diffusion in a medium-range forecast model. Mon. Weather Rev. 124, 2322–2339.

Hong, S.-Y., Dudhia, J., Chen, S.-H., 2004. A revised approach to ice microphysical processes for the bulk parameterization of clouds and precipitation. Mon. Weather Rev. 132, 103–120.

Hong, S.-Y., Noh, Y., Dudhia, J., 2006. A new vertical diffusion package with an explicit treatment of entrainment processes. Mon. Weather Rev. 134, 2318–2341.

Hsiao, L.F., Liou, C.S., Yeh, T.C., Guo, Y.R., Chen, D.S., Huang, K.N., Terng, C.T., Chen, J.H., 2010. A vortex relocation scheme for tropical cyclone initialization in advanced research WRF. Mon. Weather Rev. 138, 3298–3315.

Hsu, M.H., Fu, J.C., Liu, W.C., 2003. Flood routing with real-time stage correction method for flash flood forecasting in the Tanshui River, Taiwan. J. Hydrol. 283, 267–280.

Janjic, Z.I., 1994. The step-mountain eta coordinate model: further developments of the convection, viscous sublayer and turbulence closure schemes. Mon. Weather Rev. 122, 927–945.

Kain, J.S., Fritsch, J.M., 1990. A one-dimensional entraining/detraining plume model and its application in convective parameterization. J. Atmos. Sci. 47, 2784–2802.

Kain, J.S., Weiss, S.J., Levit, J.J., Baldwin, M.E., Bright, D.R., 2006. Examination of convection-allowing configurations of the WRF model for the prediction of severe convective weather: the SPC/NSSL Spring Program 2004. Weather Forecast. 21, 167–181.

Kain, J.S. et al., 2008. Some practical considerations regarding horizontal resolution in the first generation of operational convection-allowing NWP. Weather Forecast. 23, 931–952.

Krishnamurti, T.N., Correa-Torres, R., Rohaly, G., Oosterhof, D., 1997. Physical initialization and hurricane ensemble forecasts. Weather Forecast. 12, 503–514.

Lee, T.H., Chang, J.L., Tsai, H.C., 2000. Flood forecast system model for Tanshui River basin (I): climatology typhoon quantitative precipitation forecast model. In: Proc. Fourth Int. Conf. on Hydroinformatics, Iowa City, IA, Amer. Geophys. Union, F.1.

Li, M.H., Yang, M.J., Soong, R., Huang, H.L., 2005. Simulating typhoon floods with gauge data and mesoscale-modeled rainfall in a mountainous watershed. J. Hydrometeor. 6, 306–323.

Lorenz, E., 1963. Deterministic nonperiodic flow. J. Atmos. Sci. 20, 130–141.

Murphy, J.M., 1990. Assessment of the practical utility of extended range ensemble forecasts. Quart. J. Roy. Meteor. Soc. 116, 89–125.

Park, K., Zou, X., 2004. Toward developing an objective 4DVAR BDA scheme for hurricane initialization based on TPC observed parameters. Mon. Weather Rev. 132, 2054–2069.

Schaefer, J.T., 1990. The critical success index as indicator of warning skill. Weather Forecast. 5, 570–575.

Shih, D.S., Yeh, G.T., 2011. Identified model parameterization, calibration and validation of the physically distributed hydrological model, WASH123D in Taiwan. J. Hydrol. Eng. 16 (2), 126–136.

Simpson, R.H., 1974. The hurricane disaster-potential scale. Weatherwise 27, 169.

Skamarock, W.C., Klemp, J.B., Dudhia, J., Gill, D.O., Barker, D.M., Duda, M.G., Huang, X.Y., Wang, W., Powers, J.G., 2008. A Description of the Advanced Research WRF Version 3. NCAR Tech. Note TN-475STR, 113p.

Snyder, A.D., Pu, Z., Zhu, Y., 2010. Tracking and verification of east Atlantic tropical cyclone genesis in the NCEP global ensemble: case studies during the NASA African monsoon multidisciplinary analyses. Weather Forecast. 25, 1397–1411.

Tao, W.-K., Simpson, J., Baker, D., Braun, S., Chou, M.D., Ferrier, B., Johnson, D., Khain, A., Lang, S., Lynn, B., Shie, C.L., Starr, D., Sui, C.H., Wang, Y., Wetzel, P., 2003. Microphysics, radiation and surface processes in the Goddard Cumulus Ensemble (GCE) model. Meteor. Atmos. Phys. 82, 97–137.

Torn, R.D., Davis, C., 2012. The influence of shallow convection on tropical cyclone track forecasts. Mon. Weather Rev. 140, 2188–2197.

Tribbia, J.J., Baumhefner, D.P., 1988. The reliability of improvements in deterministic short-range forecasts in the presence of initial state and modeling deficiencies. Mon. Weather Rev. 116, 2276–2288.

Weisman, M.L., Skamarock, W.C., Klemp, J.B., 1997. The resolution dependence of explicitly modeled convective systems. Mon. Weather Rev. 125, 527–548.

Weisman, M.L., Davis, C., Wang, W., Manning, K.W., Klemp, J.B., 2008. Experiences with 0–36-h explicit convective forecasts with the WRF-ARW model. Weather Forecast. 23, 407–437.

Yamaguchi, M., Sakai, R., Kyoda, M., Komori, T., Kadowaki, T., 2009. Typhoon ensemble prediction system developed at the Japan Meteorological Agency. Mon. Weather Rev. 137, 2592–2604.

Yang, M.-J., Jou, B.J.D., Wang, S.C., Hong, J.S., Lin, P.L., Teng, J.H., Lin, H.C., 2004. Ensemble prediction of rainfall during the 2000–2002 Mei-Yu seasons: evaluation over the Taiwan area. J. Geophys. Res. 109, D18203. http://dx.doi.org/10.1029/2003JD004368.

Yang, M.J., Zhang, D.L., Huang, H.L., 2008. A modeling study of Typhoon Nari (2001) at landfall. Part I: Topographic effects. J. Atmos. Sci. 65, 3095–3115.

Yeh, G.T., Cheng, H.P., Cheng, J.R., Lin, J.H., 1998. A numerical model to simulate flow and contaminant and sediment transport in watershed systems (WASH12D). Technical Rep. CHL-98-15, Waterways Experiment Station, U.S. Army Corps of Engineers, Vicksburg, MS 39180-6199.

Yeh, G.T., Shih, D.S., Cheng, J.R.C., 2011. An integrated media, integrated processes watershed model. Comput. Fluids 45, 2–13.

Zhang, Y., Smith, J.A., 2003. Space–time variability of rainfall and extreme flood response in the Menomonee River basin, Wisconsin. J. Hydrometeor. 4, 506–517.